Extended Abstracts of the 2013 International Conference on Solid State Devices and Materials, Fukuoka, 2013, pp740-741

D-6-3

Influence of work function variation in a metal gate on fluctuation of current-onset voltage for undoped-channel FinFETs

T. Matsukawa, Y.X. Liu, K. Endo, J. Tsukada, H. Yamauchi, Y. Ishikawa, S. O'uchi, W. Mizubayashi, H. Ota, S. Migita, Y. Morita and M. Masahara

Nanoelectronics Research Institute, National Institute of Advance Industrial Science and Technology (AIST)
1-1-1 Umezono, Tsukuba, Ibaraki, 305-8568, Japan Phone: +81-29-861-5358 E-mail: t-matsu@aist.go.jp

Abstract

Influence of work function variation (WFV) in metal gates (MGs) on current-onset voltage (COV) fluctuation is investigated in detail for FinFETs. In comparison to the amorphous TaSiN MG with well-suppressed WFV, the poly-crystalline TiN MG exhibits anomalous COV fluctuation for the nMOS FinFETs. Origin of the anomalous COV fluctuation is discussed with regard due to the WFV of the TiN grains.

1. Introduction

Variability of transistor characteristics now becomes critical obstacle for further shrinkage of transistor dimensions [1]. In addition to V_t variability commonly utilized for benchmarking various technologies [1], significant fluctuation of current-onset voltage (COV), which is defined as difference between the V_t values at sub-threshold and strong inversion conditions, was revealed to be caused by random dopant fluctuation (RDF) of bulk-planar MOSFETs [2]. The COV fluctuation can be suppressed in FD-SOI MOSFETs with an undoped channel by eliminating the RDF [3]. To suppress short channel effect and V_t variability of the bulk planar MOSFETs, FinFETs with metal gates (MGs) have been introduced from 22 nm technology [4]. In this work, the COV fluctuation was examined comprehensively for the undoped-channel FinFETs with MGs. Since the V_t variability of the undoped channel FinFETs is dominantly determined by the work function variation (WFV) of the MGs [5], we compare the MGs with different WFV, namely poly-crystalline TiN and amorphous TaSiN MGs. Comparing the n/pMOS FinFETs with these MGs, the origin of the COV fluctuation is discussed in detail.

2. Sample FinFET fabrication

The MG-FinFETs are fabricated by a gate first process [5] as follows. TaSiN is used as an amorphous MG because of its thermal stability [6] together with a poly-crystalline TiN MG for comparison. After fabricating (110) fin channels from nearly undoped SOI wafers, the TiN and TaSiN MGs were deposited by sputtering on the gate dielectrics of 2 nm-thick thermal oxide. Doped poly-Si was deposited on the MGs and was used as a hard mask in the gate patterning process. Cross section of the fin channel is shown in Fig.1. While the poly grains are recognized for the TiN MG, the amorphous TaSiN MG is precisely formed on the fin sidewalls without granular morphology.

3. Variability characterization

V_g-I_d curves in the saturation region (V_d=1 V) for the FinFETs with an identical design (L_g=70 nm) are compared between the TiN and TaSiN MGs (Fig.2). The amorphous TaSiN MG exhibits smaller fluctuation of V_g-I_d curves than the TiN MG does. Pelgrom plot is obtained by measuring V_t mismatch of the paired transistors to examine the local variability (Fig.3). Amorphous TaSiN suppresses V_t variability effectively thanks to the suppressed WFV. The n and pMOS FinFETs exhibit almost identical variability for both the TiN and TaSiN MGs. Namely, the V_t variability does not depend on the channel type but on the WFV of the MGs. The A_{Vt} values obtained from the slope of the Pelgrom plot are summarized in Fig.4. Saturation characteristics ($|V_d|$=1 V) give increased variability with regard to those at $|V_d|$=50 mV due to the contribution of the DIBL fluctuation as reported in ref. [7].

Fluctuation of the COV is analyzed based on the following definitions. Representing the sub-threshold condition, V_t defined by constant current criteria (V_g at $I_d=(W_g/L_g)\mathrm{x}10^{-8}$ A) is denoted as V_{tc} [8]. Representing strong inversion, extrapolation of the maximum slope line of V_g-$I_d^{1/2}$ in the saturation region is used and is denoted as V_{tex}. The COV value is given by V_{CO}≡V_{tex}-V_{tc}. Correlation between V_{tc} and V_{tex} for the identical design (L_g=70 nm) and for $|V_d|$=1 V is shown in Fig.5. The TiN-MG nMOS case exhibits significant deviation of the plots from the regression line in comparison to the other cases. In order to analyze the deviation quantitatively, the COV statistics are summarized in Fig.6. In case of the nMOS FinFETs, the TiN MG exhibits significantly larger fluctuation of the COV than the TaSiN MG does. In case of the pMOS FinFETs, on the other hand, the fluctuation for the TiN MG is suppressed to be comparable to the TaSiN case.

In order to discuss the origin of the anomalous COV fluctuation for the TiN nMOS case, correlation between the COV and DIBL fluctuation was first examined (Fig.7). There is no significant correlation for all the cases. Thus, we consider DIBL is not the origin of the different behavior of the COV fluctuation. As reported for bulk-planar MOSFETs, a localized potential valley reflecting the non-uniformly distributed dopants in the channel causes anomalous leak current in the sub-threshold condition, resulting in COV fluctuation [2,8]. Similarly, the WFV of the MG causes the potential non-uniformity even in the undoped channel [5,9]. The TiN MG film used for the FinFET exhibits dominant orientation of (100) (Fig.8). It is reported that the dominant (100) grains have WF of 4.6 eV whereas subdominant (111) grains have lower WF of 4.4 eV [10,11]. Fig.9 shows the explanation for the anomalous COV fluctuation of the TiN nMOS case. In the nMOS case, the low-WF grain causes localized potential valley for electrons at the source edge, resulting in the anomalous leak current. In the pMOS case, on the other hand, the dominant high-WF grains determine the bottom of potential for holes and the localized potential increase due to the high-WF grain negligibly affects the leak current. In the case of the amorphous TaSiN MG with well-suppressed WFV, the leak current is not influenced by the potential non-uniformity both for the n and pMOS cases. Benchmarking of the COV fluctuation with regard to the bulk planar MOSFETs [8] is summarized in Fig.10. Generally, the MG FinFETs with the undoped channel exhibit smaller COV fluctuation due to RDF reduction. Anomalous COV fluctuation due to the WFV can be suppressed by using the amorphous MG with well-suppressed WFV.

4. Conclusion

The COV fluctuation is analyzed for the undoped-channel FinFETs with poly-crystalline TiN and amorphous TaSiN MGs. The TiN nMOS case exhibits anomalously large fluctuation of the COV in comparison to the other cases. This COV fluctuation is caused by the WFV due to the poly-grains of TiN and can be suppressed by using the amorphous MG with well-suppressed WFV.

References

[1] K.J. Kuhn *et al.*, *IEEE T-ED*, 58, p.2197 (2011). [2] T. Tsunomura *et al.*, *VLSI Symp.*, p.97, (2010). [3] T. Hiramoto *et al.*, *SOI Conf.*, p.170, (2010). [4] C. Auth *et al.*, *VLSI Symp.*, p.131 (2012). [5] T. Matsukawa et al., *IEDM*, p.175, (2012). [6] Y.-S. Suh *et al.*, *J. Vac. Sci. Technol.*, B22, p.175 (2004). [7] O. Weber *et al.*, *IEDM*, p.245 (2008). [8] T. Tsunomura *et al.*, *Jpn. J. Appl. Phys.*, 50. p.04DC08, (2011). [9] X. Wang et al., *IEDM*, p.103, (2011). [10] A. Yagishita *et al.*, *IEEE T-ED*, 48, p.1604 (2001). [11] K. Nakajima *et al.*, *VLSI Symp.*, p.95 (1999).

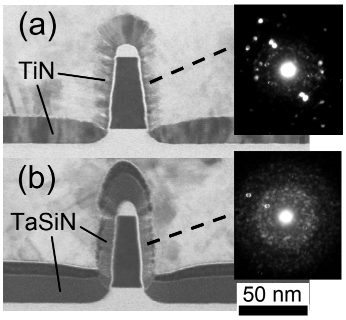

Fig.1 Cross sectional TEM and nano-beam diffraction analysis of (a) TiN and (b) TaSiN MG FinFETs. Amorphous TaSiN is precisely formed on the fin sidewalls.

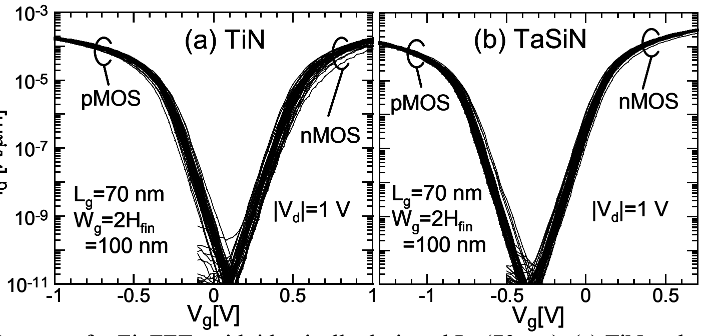

Fig.2 Fluctuation of V_g-I_d curves for FinFETs with identically designed L_g (70 nm). (a) TiN and (b) TaSiN MGs. The amorphous TaSiN MG significantly suppresses fluctuation of V_g-I_d curves.

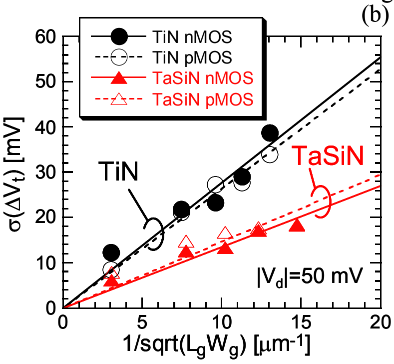

Fig.3 Pelgrom plot for TiN and TaSiN MG FinFETs. Amorphous TaSiN MG suppresses V_t variation both for the n- and pMOS FinFETs.

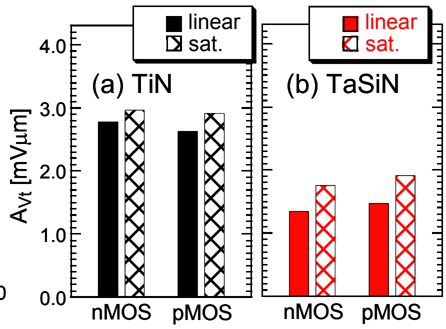

Fig.4 A_{Vt} values for TiN and TaSiN gated FinFETs in linear ($|V_d|$=50 mV) and saturation ($|V_d|$=1 V) conditions. Increased variability for $|V_d|$=1 V is caused by DIBL fluctuation.

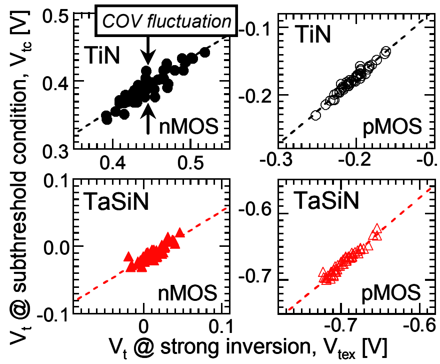

Fig.5 Correlation between V_{tc} and V_{tex} for designed L_g of 70 nm and $|V_d|$=1 V. Dotted lines show regression of the correlation.

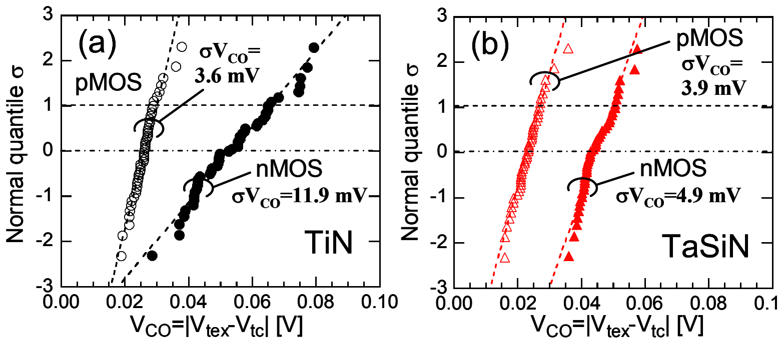

Fig.6 Statistical distribution of COV for (a) TiN and (b) TaSiN MG FinFETs. TiN-MG nMOS FinFETs exhibit anomalous fluctuation of the COV.

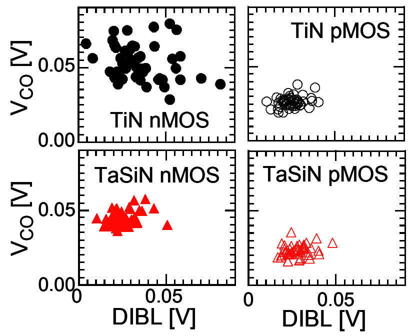

Fig.7 Correlation between COV and DIBL fluctuation. No significant correlation is not recognized.

Orientation	WF [eV]
TiN(100)	**4.6**
TiN(111)	4.4

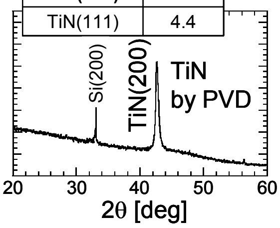

Fig.8 XRD curve of the TiN film used in the FinFETs showing dominant orientation of (200). Work function values reported for TiN with (100) and (111) orientation [10,11].

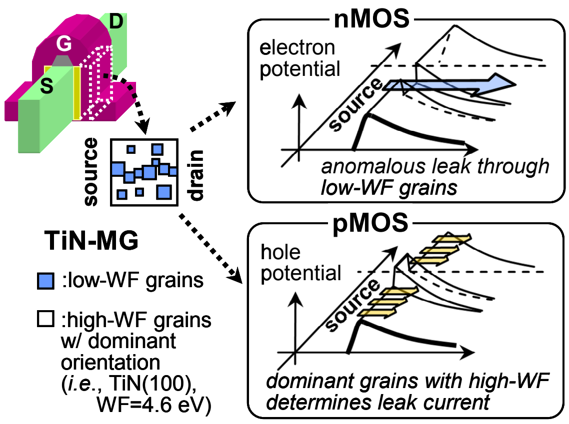

Fig.9 Explanation for the anomalous COV fluctuation of the TiN-MG nMOS FinFETs due to WFV.

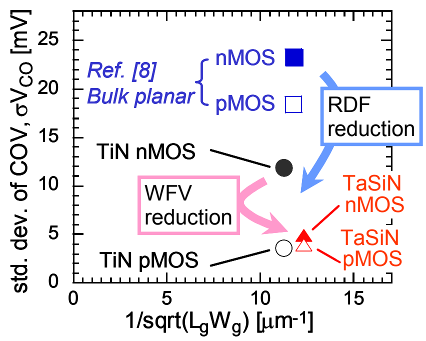

Fig.10 Benchmarking of COV fluctuation for MG-FinFETs with regard to those for bulk-planar MOSFETs [8].